IET Generation, Transmission & Distribution

WILEY

IET The Institution of Engineering and Technology

ORIGINAL RESEARCH OPEN ACCESS

Predicting Flexibility From LV Networks by Using Geospatial Forecasting and Synthetic Network Models

Giuditta Pisano | Fabrizio Pilo | Simona Ruggeri

Department of Electrical and Electronic Engineering, University of Cagliari, Cagliari, Italy

Correspondence: Giuditta Pisano (giuditta.pisano@unica.it)

Received: 30 December 2025 | **Revised:** 21 April 2026 | **Accepted:** 29 April 2026

ABSTRACT

The flexibility provided by distributed energy resources and demand response can increase the capacity of existing distribution networks to accommodate renewable energy generation and new high-peak/coincident loads. However, the use of flexibility in providing local services to distribution system operators can limit the availability of flexibility for system ancillary services, which are necessary for the transmission system operator to ensure security and adequacy. Since flexibility is not infinite, the competition between the system operators will increase with the progression of the energy transition. The same interaction appears between medium-voltage and low-voltage grids, for instance, when smaller distribution system operators are supplied by medium-voltage distribution networks operated by a different distribution system operator. The secondary substation, the interface between the medium-voltage and the low-voltage, can provide ancillary services by changing its working point to keep the operation of the medium-voltage network within technical boundaries. Forecasting the secondary substation behaviour is not straightforward due to the lack of information on low-voltage networks and generation/consumption patterns. The paper proposes a methodology to estimate and forecast the flexibility that low-voltage distribution networks can provide, even when detailed data about these networks is missing. The proposed method combines the geospatial forecasting, useful for estimating demand, generation, and resource distribution using geographic and demographic data; the synthetic low-voltage network modelling, for creating realistic network models when detailed data is unavailable; and the flexibility estimation at the secondary substation for determining how its operating point can be adjusted to provide services to the medium-voltage grid while complying with the low-voltage network constraints. The proposed approach is validated by evaluating suitable grid operation metrics, such as technical constraint violations, hours of violations, Monte Carlo convergence criteria, required low-voltage reinforcements, and the resulting feasible flexibility at the medium/low-voltage interface across multiple future scenarios through exemplary case studies that demonstrate its efficacy.

1 | Introduction

The motivation of this work is related to the increasing penetration of renewable energy sources (RES) and the electrification of final energy uses, which are profoundly impacting the power distribution system. An increasing share of new renewable generation and emerging loads, such as electric vehicle (EV) charging, heat pumps and induction stoves, are connected to medium and low-voltage (MV, LV) networks, which are already facing capacity shortages and issues in voltage regulation, congestion,

Abbreviations: DER, distributed energy resources; DG, distributed generation; DR, demand response; DSO, distribution system operators; EV, electric vehicle; GIS, geographic information system; HCS, home charging station; HV, high voltage; LP, load profile; LV, low-voltage; MV, medium-voltage; OL, overload; OPF, optimal power flow; OT, overtemperature; OV, overvoltage; PF, power flow; PV, photovoltaic; RES, renewable energy sources; RN, representative network; SS, secondary substation; TSO, transmission system operator; UV, undervoltage.

imbalance, and power quality [1, 2]. The investments required to adapt distribution networks to this transition are expected to be substantial. Furthermore, they must be planned under significant uncertainty regarding the pace and spatial distribution of electrification [3]. The resort to flexibility (i.e., the capability and willingness to deviate from their regular operating pattern in response to external signals) from distributed energy resources (DERs) and demand response (DR) can increase the capacity of existing distribution networks to accept renewable generation and new high-peak/coincident loads, postponing capital expenditures without reducing the pace of energy transition, as confirmed by the recent literature [4–6]. In the EU, prior to the EU Directive 944 [7], distribution system operators (DSOs) were not permitted to purchase flexibility services, and similar limitations were applied worldwide by many regulations. As a consequence, the most significant research and development efforts have been motivated to focus on regulating flexibility for system ancillary services. With the new role of DSOs, interest also lies in determining the necessary flexibility in distribution systems for local ancillary services and for interactions with the transmission system operator (TSO) activities. Indeed, the use of flexibility by DSOs can limit the availability of flexibility for system ancillary services, which are necessary for the TSO to ensure system security and adequacy. Thus, TSO/DSO interaction is crucial; however, since flexibility is limited, the risk of competition can increase as the energy transition progresses [8]. Since large amounts of flexibility are allocated in LV networks, interaction within the distribution system is also crucial, due to the mutual influence between MV and LV. This is particularly true when smaller DSOs are supplied by MV distribution networks operated by a different DSO, but even when there is a single DSO, similar issues arise when LV flexibility is used to meet upper-level needs.

In all these cases, the boundary is the secondary substation (SS), which can be modelled as a four-quadrant equivalent generator capable of adjusting its working point to maintain the operation of the MV network within technical boundaries [9]. Forecasting SS behaviour is not straightforward due to the limited available information on LV networks and generation/consumption patterns. Accordingly, many DSOs are investing in digitalisation programmes [10, 11]. Until enriched datasets become complete and homogeneous across the territory, however, planning studies still need to rely on proxy models derived from available GIS information and open geospatial data, such as synthetic LV network models built from street maps, building footprints, and customer locations [12–14].

From the literature review emerges that several authors have started to link flexibility provision with the technical limitations of distribution grids [15–17]. A large body of work focuses on the coordination between TSOs and DSOs and on the characterisation of flexibility at TSO–DSO boundary nodes. However, these analyses are generally limited to a small number of distribution networks, often based on IEEE test systems rather than on networks representative of real operating conditions, and therefore do not provide a scalable framework applicable to large numbers of substations [15, 17], which is instead a key feature of the methodology proposed in this paper. In [15], for instance, the Authors propose a grid-structure optimisation technique to estimate feasibility and flexibility regions at the TSO–DSO interface and tested on modified IEEE 9 and 33 bus systems. Also in [17], the available flexibility area of active distribution networks at the TSO–DSO interface is estimated using an aggregated network model, and the authors tested it in a single distribution grid case. In [16] a grid-aware framework combines a detailed MV model with a measurement-based LV representation to derive fast and slow flexibility capability curves at the primary substation, relying on extensive LV monitoring and a limited set of real feeders. However, the LV system is represented through sensitivity coefficients rather than through explicit network studies, thus limiting the detailed characterisation of actual LV grid conditions. By contrast, the methodology proposed in this paper relies on explicit LV network modelling and enables scalable analysis across thousands of secondary substations using representative synthetic network models bridging a literature gap without posing scalability issues in large scale application.

For LV system modelling, synthetic network modelling and data-driven approaches have been proposed mainly for hosting capacity and planning studies rather than for flexibility at the MV/LV interface [18–20]. Tools such as [18] and [19] generate LV synthetic grid data from open geospatial information, while [20], uses a model-free three-phase OPF based on smart-meter and transformer data without coupling to long-term geospatially downscaled scenarios. However, these approaches neither explicitly address the estimation of upward and downward flexibility exchanged with the MV grid nor couple LV modelling with long-term geospatially downscaled scenarios. In contrast, this paper specifically addresses these aspects by combining representative synthetic LV network models with scenario-based geospatial downscaling, so as to quantify the flexibility that LV systems can make available to the upstream MV network at scale.

This paper proposes a methodology based on the concept of synthetic network models to identify and forecast the amount of LV flexibility that does not create technical issues to the LV system itself. First, before modelling real networks with synthetic models, global projections formulated at national or regional levels are downscaled to the LV level to estimate expected demand, generation, and EV diffusion under future growth scenarios. In the absence of information on LV systems, the land-use characteristics of the territory served by the studied SS are used to generate geospatial forecasts of load and generation patterns. Then, by matching the real networks with a small number of representative ones, obtained by classifying real LV networks into classes based on SS macro-parameters and selecting, for each class, the network closest to the class-average electrical indicators, according to the rule-based technique described below, the synthetic network models underlying each MV/LV node (i.e., the SS) are identified. Different scenario-dependent network variants of these synthetic network models are further defined to represent the evolution of real networks under future scenarios. Finally, by performing unbalanced load flow calculations on the synthetic network models, a preliminary check is made to verify whether the networks can tolerate the demand and generation growth imposed by the scenarios. In positive cases, the potential flexibility is assessed by hypothesising a reasonable level of participation of prosumers and customers. Otherwise, the LV network is counted among those that require reinforcements to restore compliance, and, **o**nce compliance is ensured, the potential flexibility is finally assessed. The feasibility of offering the full potential flexibility to the MV grid (i.e., the maximum offers calculated for upward

and downward variations) is verified through additional network calculations. If criticalities in the LV network are identified, the feasible flexibility is reduced until no violations occur.

The validity of the approach is demonstrated in the paper by evaluating, through exemplary case studies, suitable grid operation metrics, such as technical constraint violations, hours of violations, Monte Carlo convergence criteria, required low-voltage reinforcements, and the resulting feasible flexibility at the medium/low-voltage interface across multiple future scenarios.

1.1 | Extensions With Respect to the Conference Version

A preliminary version of this work was presented in [21]. The present journal manuscript significantly extends and improves the original contribution in several dimensions, summarised below.

1. The description of LV network modelling has been enhanced. While the conference paper introduced the general concept of representative networks and synthetic models, this journal version provides a more rigorous and detailed procedure for their construction, including the definition of classification criteria, the selection of representative networks based on electrical indicators, and the generation of scenario-dependent network variants.
2. The treatment of future scenarios has been significantly expanded. The journal version introduces a comprehensive geospatial downscaling methodology that allocates demand, distributed generation, and electric vehicle charging to each SS using GIS-based techniques and land-use information. This allows for a more realistic, spatially consistent representation of the evolution of LV networks.
3. The assessment of network operation has been improved by detailing the probabilistic framework based on Monte Carlo simulations of unbalanced power flows. This is to better validate the proposed evaluation of technical constraint violations (voltage limits, line and transformer loading) under uncertainty, which was only partially described in the conference version.
4. This work explicitly quantifies LV network reinforcement needs and integrates them into the flexibility assessment. The impact of reinforcements on restoring network feasibility and increasing the amount of deliverable flexibility at the MV/LV interface is analysed, together with an estimation of the associated investment costs.
5. The analysis of flexibility has been extended from aggregate indicators to a detailed evaluation of feasible flexibility at the SS level, explicitly accounting for LV technical constraints. The results highlight how network limitations can significantly reduce the theoretical flexibility potential, providing new insights that were not covered in the preliminary contribution.
6. Finally, the overall methodological workflow has been considerably expanded and clarified, ensuring full reproducibility of the proposed approach and enabling its application to large-scale distribution systems.

The structure of the paper is as follows. Section 2 describes the main models adopted, including scenario definition and projection, the synthetic models of LV networks, and the flexibility providers. Section 3 presents the proposed five-step approach for estimating the flexibility that LV networks can offer. Section 4 presents the application to a regional distribution system and discusses the main numerical results in terms of LV criticalities, reinforcement needs, and feasible flexibility at the MV/LV interface. Section 5 concludes the paper and outlines directions for future research.

2 | Models

Many uncertainties affect flexibility estimation, and the first step in managing them is to model all currently existing items as closely as possible to reality. The following paragraphs describe the proposed models of scenarios, networks, and flexibility providers.

2.1 | Scenarios

The definition of scenarios in terms of demand, generation, and EV diffusion growth for the horizon years is indispensable for estimating the potential flexibility of distribution networks. Unfortunately, applying EU National Energy and Climate Plans, or non-European scenarios, to obtain data at the level of detail required by the distribution planning is not straightforward. For this reason, the first contribution of the paper is the definition of a scalable and replicable procedure for downscaling demand and generation high-level scenarios and forecasts to the SS level. Forecasts on EV penetration and new transportation systems are also taken into consideration. For the load demand, the developed approach is bottom-up, based on data from a defined portion of the territory, for which the characteristics of the MV nodes (i.e., SSs) in that portion are known. The considered portion of the territory should consist of the smallest area for which electrical and territorial data can be known. In this study, the province is chosen as the smallest portion of the territory due to the availability of data from previous studies [4]. By employing geospatial tools (i.e., GIS), the province is subdivided into portions of territory served by a single SS. The approach is based on the geometric procedure known as the Voronoi diagram or Thiessen polygons [4, 22]. Once the spatial distribution of SSs is known, the technique, which can be automatically implemented within a GIS environment, creates polygons around each point (i.e., each SS) so that each polygon contains the entire area that is closest to that point than any other point in the dataset, as shown in Figure 1. It is assumed that each SS serves the around territory bounded by the relevant polygon. Then, all the available data about population, land use, buildings, etc., are associated with the polygon that represents the pertinence of one SS.

Once the list and basic electrical data for the SSs in one province (i.e., the MV nodes of the distribution system) are known, the energy demand share of each SS in the province at year zero can be calculated. If no information on the types of

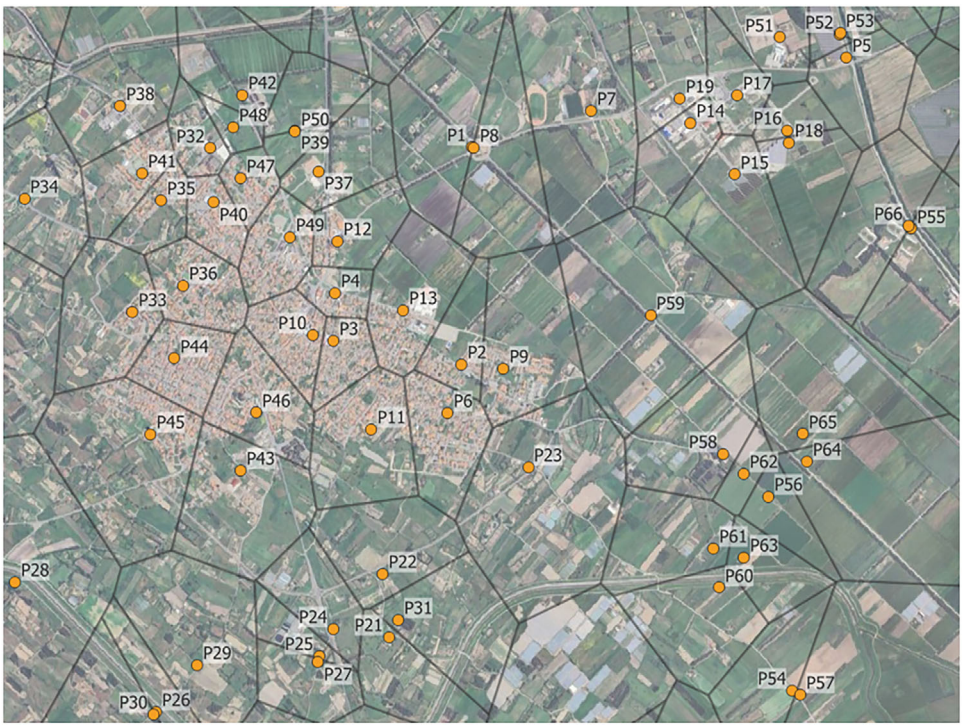

FIGURE 1 | Sample of subdivision of an area into Thiessen polygons.

customers served by the SS is available, the shares for residential, agricultural, commercial, and industrial customers can be estimated by downscaling the approach proposed by the authors in [14] for MV networks to LV networks. Such an approach considers the population, the building typology and destination use (e.g., industrial or commercial), the number of employees per commercial/industrial sector, and land cover categories to estimate demand for each end-use segment. However, in the study proposed in this paper, each MV node (i.e., each SS) is characterised by its energy demand split into residential, commercial, industrial, and agricultural sectors, as in the previous work [4], and thus the estimation was not necessary. Once the share of demand among user categories is known or estimated for each SS at year zero, and the growth rates for the future are hypothesised, it is assumed that this share remains constant over the horizon years, as projected in future scenarios. This assumption is based on the fact that projected growth is primarily driven by increased electricity consumption per user rather than by significant changes in the number of users connected to each SS. Modelling variations in user numerosity would imply network expansion and the installation of new substations, which lie beyond the scope of this work, which is focused on the evolution of existing (brownfield) networks.

Regarding the forecasted energy production from renewables, adopting the same bottom-up approach used to project demand is not reasonable. The projection of distributed generation is carried out through a top-down geospatial allocation procedure, specifically designed to overcome the limitations of purely proportional growth assumptions. In this paper, without loss of generality, only PV is considered, as it is highly prevalent in the LV. Thus, in contrast to demand, renewable generation is not projected by preserving the initial share at the SS level, as this would unrealistically assume that new capacity can be installed uniformly across the territory. Instead, the methodology distributes the expected generation by explicitly accounting for territorial constraints and hosting potential. In more detail, the total increase in generation defined at the provincial (or higher) level is allocated to each SS based on the physical and spatial characteristics of the area it serves. As mentioned, these areas are identified using GIS-based partitioning (e.g., Thiessen polygons), which associates each SS with a specific portion of territory. Within each area, the available surfaces suitable for PV installation, such as building rooftops or land for ground-mounted systems, are estimated using geospatial and land-use data. The projected generation capacity is then distributed according to the estimated hosting capacity, ensuring that installations are consistent with the actual spatial potential of each area. Furthermore, the methodology distinguishes between urban and non-urban contexts, assigning to the LV side the generation estimated for the urban context, and to the MV side the one that, for size and installation, is attributed to the non-urban context. This approach enables a spatially coherent and physically plausible projection of distributed generation, aligning large-scale scenario targets with local territorial constraints and avoiding unrealistic concentration or dispersion effects.

Regarding EV penetration, EV diffusion is projected using a geospatial downscaling procedure that allocates future transport scenarios, defined at the regional or provincial level, to individual SS, with a specific focus on the spatial distribution of charging infrastructure. The lack of reliable data at year zero required the development of an ad hoc procedure, which is based on point spatial data and evaluates the locations of EV charging stations according to the number of EVs foreseen in the scenario and the distinctive features that could characterise their owners (e.g., the possibility of installing a home charging station—HCS). The methodology first translates the expected evolution of the EV fleet into provincial-level projections, which are then

disaggregated to the local level derived from the proposed GIS-based technique (Thiessen polygons), ensuring that each SS is linked to a well-defined service area. For residential charging (i.e., HCS), the allocation is based on a bottom-up estimation of EV ownership at the SS level, derived from the share of residential customers within each substation area relative to the provincial total. This estimate is combined with building typology information and probabilistic assumptions on parking availability, allowing the calculation of the likelihood that EV owners can install private charging points (i.e., if they live in single-family houses or dwellings with shared parking lots). In this way, this methodology enables a spatially consistent projection of EV diffusion and charging demand, capturing both the heterogeneity of user behaviour and the territorial constraints affecting charging infrastructure deployment.

The procedure output allows associating the estimated demand, production, and EV charging stations with each SS of the considered territory in a future year.

2.2 | Synthetic Network Models

MV and LV distribution systems vary in many attributes across the relevant territory (e.g., topology, conductor types, transformer sizes, line lengths, load density, etc.) and often exhibit a lack of standardisation due to historical and operational reasons. Thus, extensive studies and simulations should be conducted across the territorial area under study to estimate the flexibility that LV networks can offer to the higher-voltage networks and achieve an acceptable level of confidence in the results. This paper utilises the concept of synthetic network models to address these issues and reduce the computational burden. Synthetic network models of real distribution networks do not correspond exactly to the actual networks, but they can realistically characterise them [14].

To model the real network with synthetic ones, the procedure proposed in this paper is a rule-based classification and does not apply a standard unsupervised clustering algorithm (e.g., k-means or hierarchical clustering). The objective is to reduce the number of networks that need to be explicitly simulated. In other words, the purpose of this stage is not to determine an optimal partition based on a clustering performance index, but rather to identify a limited set of LV network classes that together represent the majority of the original dataset. For this reason, and in the absence of detailed data (e.g., topology, customers, etc.) on all the LV networks to be studied, groups of LV networks with similar characteristics must be identified.

The procedure's input is the position of the SSs within the territorial area under study and a sufficiently detailed dataset for a limited number of real LV networks. In this study, about 1,000 LV networks are available with a consistent set of electrical indicators, out of the over 12,000 that serve the whole regional territory.

The real LV networks for which more details are known have been classified first into groups based on a set of macro-parameters available at the SS level. This set of parameters must also be known for the LV networks for which other details are unknown. Such macro parameters have to be accurately selected across the ones that strongly influence the topology, load density, and electrical behaviour of LV networks and are available even when detailed network models are not. For this reason, in the case study considered in this paper, the classification is performed using three macro-parameters usually available at the SS level: the rated power of the MV/LV transformer (i.e., its size); the total number of LV customers supplied by the SS; and the qualitative indicator of population concentration in the served area (high, medium, or low), derived from the municipality population according to the Italian regulatory classification (>50,000 inhabitants; 5,000–50,000 inhabitants; <5,000 inhabitants, respectively).

In particular, the dataset of known LV networks is subdivided into the typical commercial size of MV/LV transformers used in Italy for the distribution system: 50, 100, 160, 250, 400, and 630 kVA. Regarding the number of LV customers, the subdivision has been performed into three classes: fewer than 5 customers, 5–50 customers, and more than 50 customers. Considering also the classification of municipalities, each of the 1,000 known LV networks corresponds to a single parameter combination (out of the 54 possible). It is worth noting that several combinations are empty (i.e., twelve in the case study), such as those that would associate a small number of customers with a small transformer size in a densely populated municipality, and others are not very representative due to the limited cases they include (i.e., 16 combinations include fewer than ten networks). Thus, the final number of considered classes is 26.

Once the dataset of known real LV networks is subdivided into classes, other features describing the internal structure of the LV networks belonging to each class must be analysed. Each network is characterised based on a few other indicators that can characterise different behaviours within its class, that is, the average feeder length, the share of overhead lines/buried cables, the average number of customers per feeder, and the ratio of installed generation capacity to the rated power of passive customers. It is worth noting that such indicators are not available for all the LV networks that will be represented by a synthetic model, but this classification is designed to group known networks with similar structural and electrical characteristics, ensuring limited variability within each class. Another important parameter is the number of feeders that constitute the LV networks, known for the limited set of LV networks. This parameter, together with the average values of the others, guides the selection of the most representative network for each class. The representative networks (RNs) are selected to build the synthetic network model used in the simulations based on the average network characteristics and the prevailing number of feeders in each class. More in detail, the approach can be formalised as follows. Let $x_{i,k}$ be the value of the indicator k for the i-th network belonging to a given class, and $\overline{x_k}$ the average value of indicator computed over all networks in that class. The representative network RN is selected as the network that minimises the distance from the class centroid in the multidimensional indicator space, as in (1).

$$\mathrm{RN} = arg\min_i \sqrt{\sum_i \left(x_{i,k} - \overline{x_k}\right)^2} \tag{1}$$

In this way, the selected RN can be interpreted as the network whose structural characteristics are closest to the average

configuration of the class. Furthermore, the initial set of 26 representative LV networks is further analysed and compared in terms of topological and electrical characteristics. Networks exhibiting very similar features (e.g., the same number of feeders, comparable feeder lengths, and analogous configurations) are grouped together, as they would lead to equivalent results in subsequent simulations. This a posteriori aggregation reduces the initial set from 26 to 16 representative networks while preserving an adequate representation of the overall variability of the LV system. Each RN is therefore used as a synthetic model for the set of real LV networks belonging to the same class. Concerning the representativeness of the selected RNs, since their selection is made by choosing the closest-to-centroid configuration, the average deviation from all networks in the class of real LV networks for which some features were known is minimised. To further support the representativeness of the selected RNs within the limited set of LV networks, the intra-class variability of the electrical indicators has been analysed. Results show that, for each class, the dispersion of the considered indicators around the centroid is limited, confirming that each selected RN provides a reasonable approximation of the average network configuration within that class.

These RNs have therefore been assumed to represent all the LV networks under study, including those for which only the macro-parameters at the SS level are known. This approach significantly reduces the number of networks that must be analysed while preserving the diversity of network configurations present in the real distribution system. It is important to note that a full quantitative validation of the representativeness of the selected RNs over all LV networks is not feasible due to the lack of detailed data. However, the purpose of this methodology is not to provide a statistically optimal clustering of LV networks but to define a tractable set of representative configurations that can be consistently mapped to all substations based on available macro-parameters.

Once the set of RNs has been identified, each SS in the studied region is associated with its corresponding RN based on its macro-parameters, and subsequent scenario analysis and probabilistic power flow simulations are performed on these synthetic models.

To include the expected scenarios in the horizon years, modelled as in the previous paragraph, different variants of the RNs are built by crossing levels of demand, production, and EV diffusion. In this way, the number of simulations is reduced, but to not excessively lessen the accuracy of the results, a compromise between the number of selected synthetic network models and the levels of factors that characterise the future scenarios must be made. In this way, the behaviour of every real LV network is represented by its corresponding synthetic model, and, once the scenario downscaling (detailed in section 3.1) is applied, the time-varying demand and generation profiles of each SS can be combined with the assigned RN for the subsequent flexibility assessment.

Figure 2 summarises the proposed procedure for creating the synthetic network model.

Moreover, for properly considering the coincidence between demand and production, typical daily profiles (i.e., working days, pre-holidays, and holidays for the four seasons) are associated with diverse demand patterns, differentiated among the type of customers (i.e., residential, agricultural, industrial, and commercial, as in [23]), generators, and home charging stations (HCS) of each RN.

Each typical day is represented at hourly resolution and defined separately for demand and generation. Base profiles are normalised to unit daily energy and then scaled so that, for each SS and scenario year, the annual energy associated with each customer category and technology matches the values obtained from the scenario downscaling. In this way, the long-term energy scenarios are consistently translated into time-varying active and reactive power profiles that can be used in the probabilistic power flow simulations. It is worth noting that, as a result of the study in [23], different typical daily load profiles (LPs) are assigned to LV customers in a nominal homogeneous category to overcome the inaccuracy caused by non-existent coincident peaks arising from the common use of a single LP per category and per typical day. According to [23], customers supplied by the same SS (in this paper, one RN) are first grouped by annual energy consumption and geographic location, and each group is statistically associated with LP clusters through normalised distribution coefficients reflecting their relative occurrence along the network. Then, individual customers are randomly assigned to clusters based on these coefficients, and each customer is finally associated with the LP corresponding to the centroid of the selected cluster. The proposed approach overcomes the simplified approach commonly adopted in practice when detailed LV information is missing, in which the secondary-substation load profile is distributed across all downstream users proportionally to their rated power, without differentiating customer behaviour. While simple, this approach tends to produce unrealistically coincident peaks and fails to capture the diversity of LV customer demand. In Italy, the procedure for assigning time-varying power profiles to LV customers, as suggested by the Italian Regulator and used by the DSOs, starts from the active power measured at an SS, typically with a 10-minute resolution. From each customer's monthly energy consumption (available for billing purposes), individual customer power profiles are derived through the following steps.

- The active power measured at the SS is integrated to compute the total monthly energy supplied to the LV network.
- Based on the monthly energy of each customer (E_C) and the total energy measured at the SS (E_{SS}), a monthly scaling factor is calculated, as in (2).

$$k_M = \frac{E_C}{E_{SS}} \tag{2}$$

- The yearly power profile of each customer is then obtained by applying the corresponding monthly scaling factors to the measured SS profile.

This procedure is inherently applicable to passive networks, as it relies solely on energy measurements of consuming customers. Moreover, it does not differentiate among customer types: all users supplied by the same SS are assumed to share the same normalised load profile shape, derived from the SS measurements.

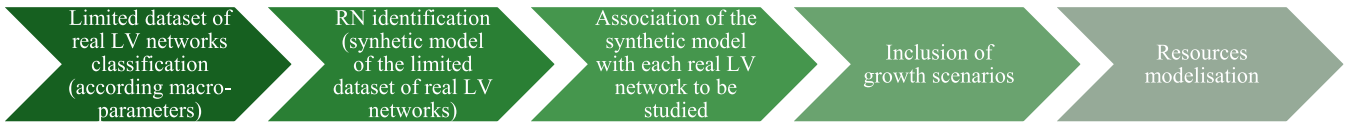

FIGURE 2 | Synthetic network model creation procedure.

On the contrary, the modelling strategy adopted in this paper provides a more realistic representation of LV demand behaviour overwhelming the conventional proportional-allocation benchmark under the same data-availability constraints.

Concerning the HCS, their charging profiles are derived from the habits of EV drivers, which allows defining average hourly consumption profiles based on vehicles and travelled distances. In detail, the online available electric vehicle charging and grid integration tool provided by the International Energy Agency (IEA) is used to generate a large number of cases for building mean daily profiles differentiated by EV model, charger power, and drivers' habits (e.g., travelled kilometres, arrival and departure time, etc.) [24]. Different charging behaviours are modelled by combining several dimensions: vehicle segment, charger power level, typical arrival and departure times, and daily driven distance. The resulting synthetic population of charging events is then mapped to the LV networks by assigning several HCS to each residential customer, according to the penetration level defined in the scenario, and by distinguishing between single-phase and three-phase connections when relevant. This procedure preserves the correlation between driving habits and the location of charging points, which is crucial for reproducing realistic coincident peaks at the feeder level [25].

2.3 | Flexibility Providers

Theoretically, all DERs can provide flexibility services: customers can reduce/increase their demand and/or shift it; owners of dispatchable generation plants can vary their production both upward and downward within the technical limits of the installed technologies; storage systems, static or mobile (i.e., EVs), can behave as a load or generator depending on their state of charge; non-programmable generators can curtail their production.

Considering all the potentiality of flexibility providers, the interface between MV and LV networks, the SS, can be modelled as a four-quadrant equivalent generator that can change its working point within a capability curve that, in the most extensive case, is a rectangle in the P-Q plane, whose vertices can be calculated as the sum of all the maximum potential offers by the DERs connected to the downstream LV network. Figure 3 shows the ideal capability curve for deviations from the expected working point (A) in each time interval.

The maximum flexibility curve is obtained by considering the maximum upward and downward bids from flexibility providers (yellow area BCDE) and disregarding the limitations of the LV grid. The assessment of such a potential can be formalised as follows. Let $\mathcal{F}$ denote the set of flexibility providers connected to a given LV network. Once the participation level for each provider $i \in \mathcal{F}$ is defined, the maximum upward and downward deviations

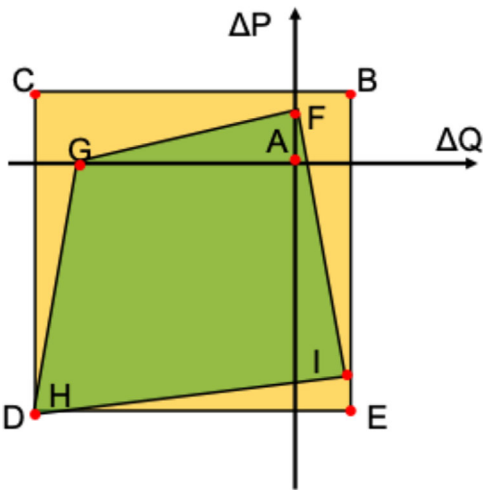

FIGURE 3 | Capability curves of the four-quadrant equivalent generator that models the SS in one time interval.

of active and reactive power, $\Delta P^{\uparrow}_{i,\max}, \Delta P^{\downarrow}_{i,\max}, \Delta Q^{\uparrow}_{i,\max}, \Delta Q^{\downarrow}_{i,\max}$, with respect to the SS expected operating point in a given time interval, can be assessed. The aggregate maximum deviations at the SS are obtained by the following (3) and (4).

$$P_{\max} = \sum_{i \in \mathcal{F}} \Delta P^{\uparrow}_{i,\max},\ P_{\min} = \sum_{i \in \mathcal{F}} \Delta P^{\downarrow}_{i,\max} \tag{3}$$

$$Q_{\max} = \sum_{i \in \mathcal{F}} \Delta Q^{\uparrow}_{i,\max},\ Q_{\min} = \sum_{i \in \mathcal{F}} \Delta Q^{\downarrow}_{i,\max} \tag{4}$$

The ideal maximum flexibility region of the SS in the P–Q plane is therefore given by all $(\Delta P,\ \Delta Q)$ that satisfy (5).

$$-P_{\min} \le \Delta P \le P_{\max}, -Q_{\min} \le \Delta Q \le Q_{\max}, \tag{5}$$

which corresponds to the area BCDE shown in Figure 3, before enforcing LV network constraints.

However, estimating the feasible flexibility cannot ignore the network operation and must keep the working point within the technical boundaries. Figure 3 shows a possible reduction of the capability area, calculated as feasible for not incurring technical constraint violations (green shape FGHI).

Since the point of view is from the LV side, customers offer upward bids when their consumption is reduced and downward bids when their demand is increased. Producers do the opposite, so that an increase in production leads to a downward bid at the SS level and a reduction in production to an upward offer. For RES generation without storage, the production increase is generally not possible. Finally, EVs and static storage systems offer downward bids in the discharging mode and upward bids in the charging phase. Thus, for instance, the point F of

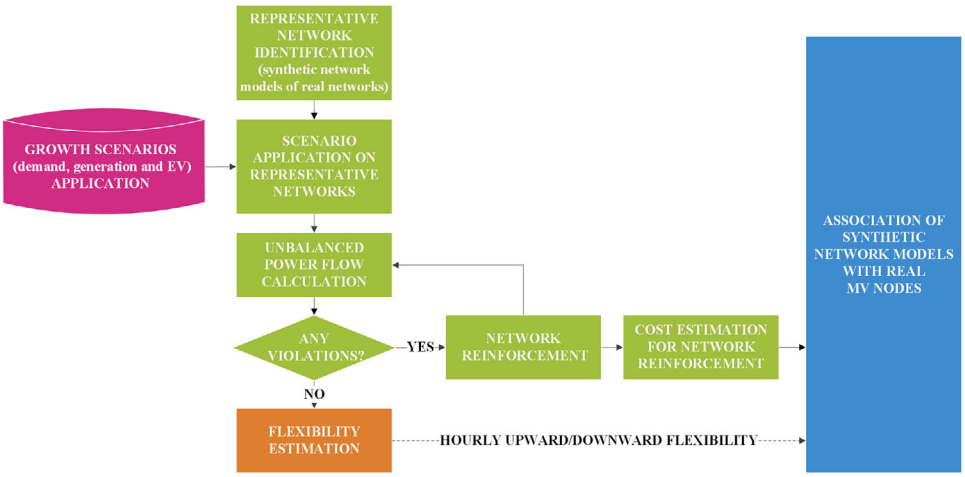

FIGURE 4 | Flow diagram of the proposed procedure.

Figure 3 represents the case when some resources cannot offer the maximum active power in upward ($\Delta P^{\uparrow} \leq \Delta P^{\uparrow}_{\max}$) and no change in reactive power is allowed ($\Delta\, Q^{\uparrow} = 0$) without violations of the technical constraints, while the point G corresponds to the case on which no change in active power ($\Delta\, P^{\uparrow} = 0$) is permitted and the reactive power can be changed in downward until a limited value, smaller than the maximum potential ($\Delta Q^{\downarrow} \leq \Delta Q^{\downarrow}_{\max}$).

3 | Proposed Approach for Assessing LV Flexibility

A five-step approach (shown in the flowchart of Figure 4) has been developed to estimate the flexibility potentially offered by the LV networks to the upper voltage level ones, and it is described as follows.

1. Identification of representative networks (RNs) that are the synthetic network models of the real ones.
2. Association of the RNs to real MV nodes, that is, the SSs, of the distribution system under study.
3. Application of a specific demand, generation and electric mobility scenario on RNs following the expected scenarios. In this step, the rules for scaling the RN to be studied are identified.
4. Unbalanced power flow (PF) calculations (using OpenDSS for 4-wire distribution systems) are performed for each RN identified in point 1 and modified, taking into account point 3, considering the following operating conditions:
   a. *As-is networks*, which represent the networks in their current configuration (i.e., year zero), are used to verify the presence of contingencies and criticalities and, if necessary, resolve them before proceeding to the next step, as outlined in point b.
   b. *Networks in horizon years* (e.g., 2030 and 2050), obtained after application of the scenarios in point 3. If the power flow calculations on the networks projected for a horizon year reveal criticalities, the necessary investments to address the detected criticalities are estimated.
5. Estimation of the flexibility that the LV network, possibly resized, could provide to networks at the upper voltage level (i.e., MV) without violating the technical constraints in its network operation.

The association of the real networks with the synthetic network models at point 2 directly derives from the classification and the rules adopted for selecting the RNs, as described in paragraph 2.2.

3.1 | Application of the Load and Generation Forecasts to the Synthetic Network Models

Concerning point 3 in Sec 3, rules for scaling these scenarios on RNs should be found to ensure that the synthetic network models can reproduce the behaviour of real networks during the expected evolution. In the following sub-paragraphs, some details of these rules are reported.

3.1.1 | Demand

Let us consider the group of real networks represented by a specific RN. This group of real networks is characterised by a certain growth in demand over the years, which results in their consumption falling within a specific range, from D_{min} (minimum demand) to D_{max} (maximum demand), in kWh/year. More in detail, by hypothesising that the group associated with a given RN includes 1000 real LV networks, each one characterised by three values of energy demand, one for the year zero and two for the two considered horizon years, 3000 values of energy demand, each associated with one combination network-scenario, are available for such a group that fall into the range D_{min}–D_{max}. The real network group is generally not evenly distributed in this range. Thus, once the group of real networks has been ordered by increasing demand growth, it has been divided into N_{D} sub-groups, each with a demand range for which the minimum, maximum, and average values can be defined. For instance, if the range D_{min}–D_{max} is between 0 to 300 MWh/year and N_{D} is assumed equal to 3, the first class is between 0–100 MWh/year, the second is between 100–200 MWh/year, and the third 200–300 MWh/year. Such classes could include a variable number of combinations of real network-scenarios. The average demand values of the identified subsets become the reference energy

TABLE 1 | Share of residential consumption across RN demand classes.

	Total demand [kWh/year]	Residential customer consumption [kWh/year]
Representative network (RN)—year 0 -	109,157	3,882
class 1	19,330	687
class 2	41,324	1,469
class 3	126,621	4,502

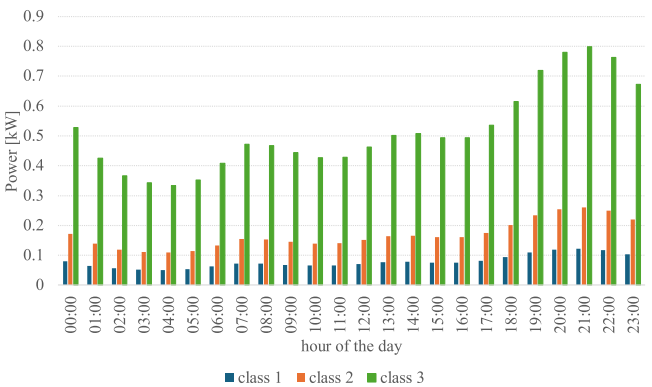

FIGURE 5 | Scaling of a daily demand profile of a residential customer of one RN in three classes.

demand of the N_D classes for each RN. In the proposed example, the average demands of the three classes are 50 MWh/year, 150 MWh/year, and 250 MWh/year, respectively. Such energy demands are then applied to the customers of the given RN, which is associated with the group of real networks, while maintaining their daily load profiles to reproduce the expected scenarios of the real networks. It is worth noting that the total energy demand applied to one RN is divided among its customers, preserving the proportionality across customer types. For instance, Table 1 shows that the residential consumption of one customer in one RN is 3,882 kWh/year, which is approximately 3.5% of the total demand. Such a share is maintained in each considered class of demand (three in this example, $N_D = 3$), and the daily profile of that customer is simply translated, as in Figure 5. The demand of one class may be smaller than of one at year zero, as in the case of class 1 and class 2 in Table 1. In any case, the daily load profiles of the customers are downscaled proportionally to their share in the real RN (Figure 5).

3.1.2 | Generation and Electric Mobility

For scaling these scenarios onto the RNs, the same rule described for demand can be applied to installed generation power and the number of HCS expected in the scenarios. Thus, N_{PV} generation classes and N_{HCS} classes for the EV charging stations can be defined. The only difference from the definition of demand classes is that classes with no PV or no HCS must also be considered if the expected scenarios do not foresee the installation of PV or HCS on the horizon years.

For positioning the generators in the RN, the generator size is determined by the type of customer connected (i.e., 3 kW for residential customers and up to 10 kW for non-residential customers). Instead, the power expected to be installed in other contexts is positioned in no-load LV nodes (up to 20 kW per node).

Regarding the HCSs, they are first positioned in nodes that supply residential customers (up to 2 HCS per customer). If the number of expected HCSs exceeds twice the number of residential customers, the remaining HCSs are randomly assigned to nodes with non-residential customers.

In summary, the networks selected as representative are at most analysed in N_D x N_{PV} x N_{HCS} versions, representing the combinations of demand, PV, and HCS classes (no PV and no HCS classes included), respectively. However, in practice, it is not necessary to build or analyse all possible combinations of classes for all RNs if none of the real networks fall into any given combination.

3.2 | Unbalanced Power Flow Calculations

Initially, power flow (PF) calculations are performed to verify if technical constraints are violated during the operation of the defined RNs. The verification is carried out using a Monte Carlo approach, in which the PF calculations are repeated by sampling demand, generation, and charging/discharging current values on an hourly basis from predefined time-dependent distributions. Specifically, a beta distribution is adopted for demand [26], while normal distributions are used for energy production and HCSs. The sampling process is based on the typical hourly profiles described in Section 2.2. The year zero and all the combinations of scenarios that reproduce the horizon years are separately simulated until the convergence criterion of the MC is met. The stop criterion for the MC cycle is reaching the maximum number of iterations or a given threshold ε to the convergence parameter β_n, calculated as in (6).

$$\beta_n = \frac{\sqrt{\sigma(h_v)}}{\mu(h_v) \cdot \sqrt{n}} \leq \varepsilon \; n = 1 \ldots N \tag{6}$$

where n is the number of the current extraction, $\sigma(h_v)$ and $\mu(h_v)$ are the variance and the mean value of the h_v occurrence of violations (expressed in hours per year) calculated until the n-th extraction. If violations are detected, a dedicated reinforcement step is triggered. First, the type and location of the issues (overvoltage, undervoltage, line or transformer overloads) are identified in each RN. For each version of RN, unbalanced power flow calculations are performed, and the resulting operating point is checked against standard technical limits, namely voltage, branch current and transformer loading constraints. Admissible operating points must satisfy the following constraints in (7).

$$\begin{gathered} V_{\min} \leq V_n \leq V_{\max} \; \forall n \\ I_{\mathcal{L}} \leq I_{\mathcal{L}}^{\max} \; \forall \mathcal{L} \\ S_{\text{tr}} \leq S_{\text{tr}}^{\max} \end{gathered} \tag{7}$$

where V_n is the voltage magnitude at node n, $I_{\mathcal{L}}$ is the current in line $\mathcal{L}$, and S_{tr} is the apparent power at the secondary substation transformer. The considered limits are $V_{\min} = 0.95$ p.u., $V_{\max} = 1.05$ p.u., $I_{\mathcal{L}}^{\max} = 100\%$, $S_{\text{tr}}^{\max} = 100\%$.

In other words, the Monte Carlo simulations adopt a risk-orientated convergence criterion based on the estimated annual duration of technical constraint violations. The convergence threshold ε is set equal to 5 h/year in the case study. At each iteration, the mean and variance of the annual violation hours are updated, and a convergence indicator is evaluated as the variation between consecutive estimates, normalised over the simulated year. The simulation process is stopped when either: (i) the convergence indicator falls below the threshold ε, indicating negligible variation in the estimated violation risk, or (ii) a predefined maximum number of iterations is reached, in order to limit computational burden. Further details on the computational aspects are provided in Section 4.3.

For thermal violations, components that exceed their overload limits are reinforced without changing the network topology. Specifically, LV cables are resized to a larger standard cross-section, and MV/LV transformers are replaced with the next available commercial rating. The new rating is chosen as the smallest standard commercial size capable of withstanding the maximum simulated loading. Voltage violations are addressed by resizing the entire feeder, which constrains the voltage profile. The costs of the selected reinforcements are then quantified according to the DSO's cost assumptions, and the resulting reinforced elements replace the original ones in the synthetic network models. The reinforced network is used in the subsequent step (point 5) to reassess operation and feasible flexibility at the MV/LV interface.

3.3 | Flexibility Estimates

Step 5 of the proposed approach is performed by considering, for each RN, possibly resized, the vertices of the rectangular capability curve in Figure 3 that determine the maximum deviations from the expected working point of the MV/LV network interface. By referring to Figure 3, starting from the expected working point A (the origin of the ΔP and ΔQ plan), the maximum variation upward can be obtained by combining the maximum reduction of the demand and the maximum charging power of static storage systems and EVs with the expected power production and the cumulative variations in positive (i.e., point E) or in negative (i.e., point D) of the reactive power of demand and the one allowed by the capability curves of the inverters used for the connection of the static and mobile storage systems. On the other hand, the maximum downward variation can be obtained by combining the maximum demand increase, the maximum discharge of static storage systems and EVs and the cumulative variations in positive (i.e., point C) or in negative (i.e., point B) of the same contributions of reactive power, with the PV shut down. It is worth noticing that the demand cannot easily change its power factor. Thus, the corresponding variation of reactive power follows the variation of the active power.

The feasibility check is carried out by running unbalanced power flow calculations on the LV network models (i.e., representative/synthetic networks) for these four relevant operating conditions. In the unbalanced power flow simulations, the slack bus is located at the MV node of the MV/LV transformer of the secondary substation, which represents the interface between the upstream MV network and the LV system under analysis. The voltage at the slack bus is assumed equal to the nominal MV voltage, consistent with the objective of the study, which focuses on assessing the technical feasibility of flexibility provision within LV networks without explicitly modelling the upstream MV grid.

The LV network can offer 100% of the potential flexibility if no violations occur. Otherwise, if any technical constraint is overcome, the deviation from the expected working point is reduced with respect to the maximum potential until a condition with no violation is found. Practically, this is implemented by progressively scaling down the deviation along the corresponding direction of the capability curve (upward or downward), while repeating the PF calculations until all voltage and thermal limits are respected. Such final percentages of upward or downward flexibility determine the feasible flexibility that the real networks, represented by the synthetic network under study, can offer to the MV.

4 | Case Study and Results

The procedure is applied to an Italian region, whose distribution system comprises about 12,000 SSs. The number of selected RNs is 16 (Figure 6 shows three of them). Their main characteristics (i.e., the number of feeders, average feeder length, share of overhead lines, number of connected customers, and the ratio of installed generation capacity at year zero -P_{active}- to the rated power of passive customers -P_{passive}-) are reported in Table 2. The last column indicates the share of the ∼12,000 real secondary substations in the region that are represented by each RN.

The long-term demand and generation scenarios are derived from a previous regional study that assessed the potential to become a green model for the energy transition, characterised by high electrification and extensive use of renewables [4]. On the demand side, the sectoral growth rates are consistent with the National Energy and Climate Plan. They are driven by increased environmental awareness, efficiency improvements, lower electricity prices due to higher RES penetration, and the deployment of local energy communities and new electricity-based technologies (e.g., hydrogen). By 2030 and 2050, electricity demand is expected to grow moderately in the residential, tertiary, and agricultural sectors, more strongly in industry, and significantly in transport due to road electrification, with EVs reaching more than 70% of the car fleet by 2050. On the generation side, the scenario assumes a mix of onshore wind and photovoltaic plants. Since wind plants are supposed to be connected to the HV system, they are not considered in this study. Whereas photovoltaic capacity is apportioned between MV and LV according to the downscaling assumptions. In urban areas, PV is modelled as LV-connected. In contrast, in non-urban areas, if the PV growth scenario for a given RN results in a cumulative rated power below 130 kW, the PV is spread throughout the LV RN, as it is LV-connected only. Otherwise, it is modelled as MV-connected.

To cover all the identified scenarios applicable to real networks for the horizon years 2030 and 2050, the selected RNs are built

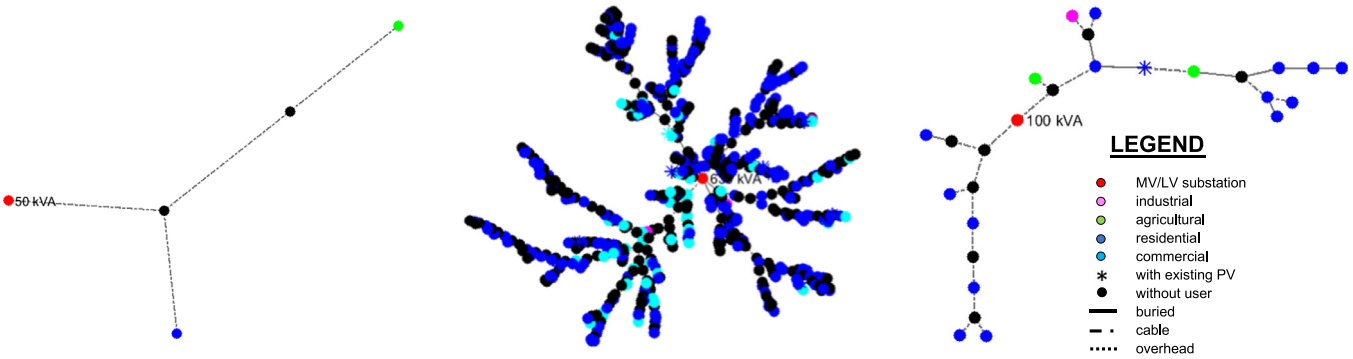

FIGURE 6 | Example of three of the LV synthetic networks used in this study.

TABLE 2 | RN main characteristics.

	Network parameters					
NETWORK ID	**Num of feeders**	**Feeder length [km]**	**Share of overhead lines**	**Number of clients**	$\mathbf{P_{active}/P_{passive}}$	**Representativeness**
RN 1	1	0,42	100%	2	0	24.8%
RN 2	2	1,42	100%	8	0,14	11,7%
RN 3	1	0,21	0%	2	0	3,7%
RN 4	2	0,50	88%	11	0,05	5,1%
RN 5	4	0,43	0%	85	0,09	11,5%
RN 6	1	1,54	83%	26	0,08	6,9%
RN 7	2	1,67	80%	110	0,06	1,3%
RN 8	2	0,35	0%	4	0	2,1%
RN 9	4	0,28	0%	22	0,20	6,8%
RN 10	2	0,29	0%	19	0,37	2,5%
RN 11	4	0,31	4%	120	0,06	3,7%
RN 12	4	0,76	4%	364	0,06	8,8%
RN 13	4	0,20	3%	61	0,03	6,4%
RN 14	8	0,97	64%	389	0,04	1,0%
RN 15	6	1,00	4%	568	0,06	2,1%
RN 16	6	0,21	5%	61	0,01	1,7%

in 469 different variants. It is worth noting that, depending on their initial energy demand, one RN-scenario combination can represent two real networks belonging to the same group of real networks represented by the given RN, one in the first horizon year and another in the second.

4.1 | Networks in Horizon Years

Preliminarily, and accordingly to step 4.b of the proposed approach (Section 3), power flow calculations on the networks projected in a horizon year are checked. If criticalities are identified, the necessary investments to address them are estimated. The criticalities vary significantly across network types, with some RNs remaining largely compliant (e.g., RN 9, RN 10, RN 13) and others showing criticalities in the majority of simulated scenarios (e.g., RN 12 and RN 14) or in all the combinations (e.g., RN 7, RN 15). Figure 7 shows the share of RN–scenario combinations that exhibit no criticalities, criticalities exceeding the threshold of five critical hours per year, and combinations where no real network falls (no scenario).

Considering all the RNs identified for this study, approximately 52% of these networks do not require resizing to address criticalities. RNs that do not require reinforcement in any combination are approximately 20% (Figure 8). The other networks must be resized to accommodate the growth in demand, production, and HCS diffusion over the horizon year. In Figure 8, the numbers within the bars indicate the number of real networks each RN represents.

Figure 9 and Figure 10 show the results of the MC simulations for three of the 16 identified RNs, considering the different levels of generation, demand, and HCS diffusion. In particular, Figure 9

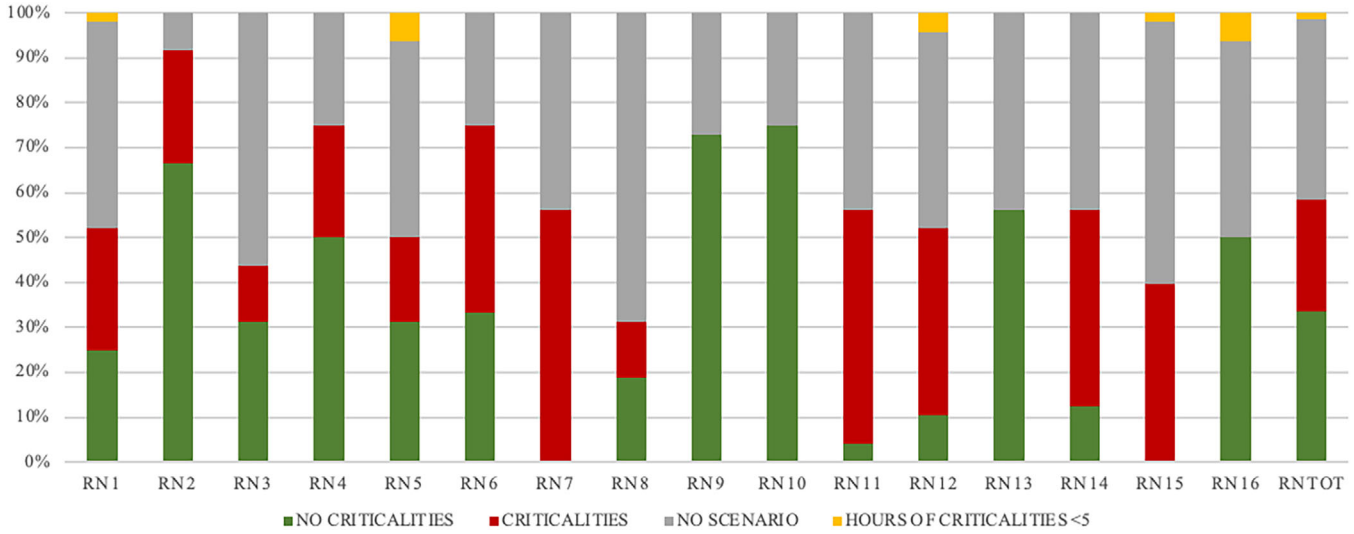

FIGURE 7 | Share of RN–scenario combinations with and without criticalities for each representative network.

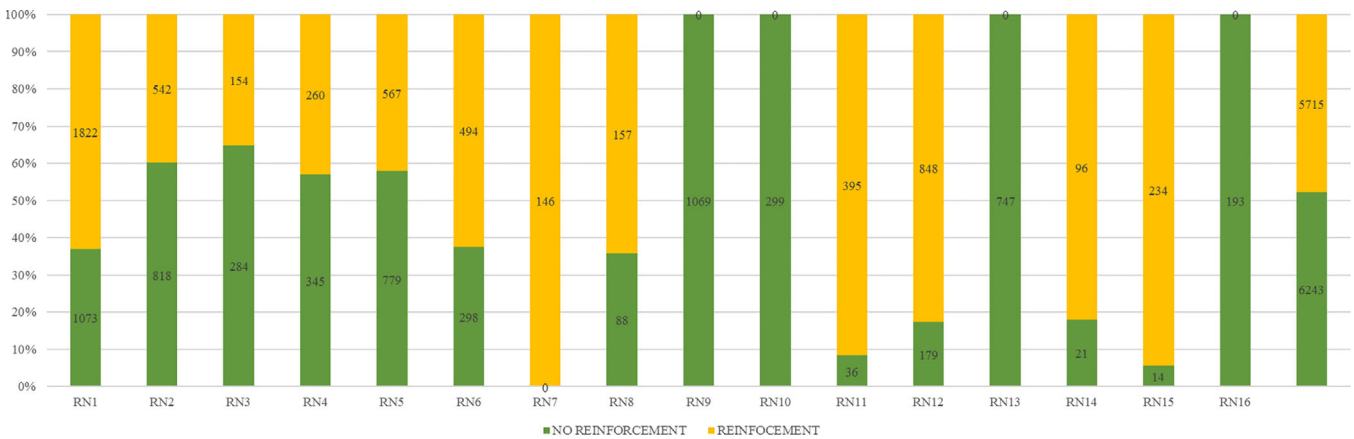

FIGURE 8 | Percentage of real networks represented by the RNs that do not/must be resized.

illustrates, using traffic lights, the presence of criticalities in the networks. Green dots indicate scenario–network combinations in which no violations are observed in any Monte Carlo sample. In contrast, red dots highlight combinations in which technical constraints are violated for more than a fixed number of critical hours (i.e., 5 h in this study). At the same time, the hyphen indicates the absence of a scenario (i.e., the RN-scenario combination does not represent any real network, not even in a future year). It is clear that criticalities emerge and become more frequent as the penetration of distributed resources increases. For example, the number of red dots increases when moving from PV class PV1 to PV3 and when demand (or HCS diffusion) rises. Figure 10 details the type of criticality registered (i.e., transformer or line overloading, OL/OT, overvoltage, OV, or undervoltage, UV) and if they happen during the day (_D) or not (_ND). The cells marked with a hyphen correspond to the absence of a given type of criticality throughout the simulated year; otherwise, the presence of OL, OV, or UV indicates that the corresponding limit is exceeded in at least one Monte Carlo sample. The grey areas correspond to the network variants not simulated. As shown in Figure 9, the variety of criticalities increases with the penetration of distributed resources. For instance, new types of criticalities emerge when demand (or HCS diffusion) increases in network RN 6.

From another perspective, Figure 11 illustrates the identified criticalities, namely overvoltage, voltage drops (undervoltage) at the nodes, and line and transformer overloading. It is subdivided into the four quarters of the year. Overloading of transformers and lines, as well as overvoltage, occurs mainly during the spring and summer quarters (i.e., Q2 and Q3). Excessive voltage drops arise throughout the year but are most prevalent during the autumn and winter quarters (i.e., Q1 and Q4). A clear distinction also emerges between network types: rural networks are mainly characterised by voltage-related criticalities, often coupled with daytime line current violations, whereas urban networks are more frequently affected by thermal congestion and equipment overloading. In quantitative terms, nearly 50% of the analysed networks exhibit current violations, 47% present voltage violations, and 17% show transformer overloading.

RN/HCS		HCS0			HCS1			HCS2			HCS3		
		D1	D2	D3	D1	D2	D3	D1	D2	D3	D1	D2	D3
RN 6	PV0	-	-	-	-	-	-	-	-	-	-	-	-
	PV1	🟢	🟢	🔴	🟢	🟢	🔴	🟢	🟢	🔴	🟢	🟢	🔴
	PV2	🟢	🟢	🔴	🟢	🟢	🔴	🟢	🟢	🔴	🟢	🟢	🔴
	PV3	🔴	🔴	🔴	🔴	🔴	🔴	🔴	🔴	🔴	🔴	🔴	🔴
RN 10	PV0	-	-	-	-	-	-	-	-	-	-	-	-
	PV1	🟢	🟢	🟢	🟢	🟢	🟢	🟢	🟢	🟢	🟢	🟢	🟢
	PV2	🟢	🟢	🟢	🟢	🟢	🟢	🟢	🟢	🟢	🟢	🟢	🟢
	PV3	🟢	🟢	🟢	🟢	🟢	🟢	🟢	🟢	🟢	🟢	🟢	🟢
RR 14	PV0	-	-	-	-	-	-	-	-	-	-	-	-
	PV1	-	-	-	🟢	🟢	🔴	🟢	🔴	🔴	🔴	🔴	🔴
	PV2	-	-	-	🟢	🟢	🔴	🟢	🔴	🔴	🔴	🔴	🔴
	PV3	-	-	-	🔴	🔴	🔴	🔴	🔴	🔴	🔴	🔴	🔴

FIGURE 9 | Traffic-light summary of the presence/absence of technical criticalities for three representative LV networks under different scenario combinations.

RN/HCS		HCS0			HCS1			HCS2			HCS3		
		HCS0	D2	D3	D1	D2	D3	D1	D2	D3	D1	D2	D3
RR 6	PV0												
	PV1	-	-	UV	-	-	UV	-	-	UV	-	-	UV
	PV2	-	-	UV	-	-	UV	-	-	UV	-	-	UV
	PV3	OV + OL_D + OT_D	OV + OL_D + OT_D	UV + OV + OL_D + OT_D	OV + OL_D + OT_ND + OT_D	OV + OL_D + OT_ND + OT_D	UV + OV + OL_D + OT_D	OV + OL_D + OT_D	OV + OL_D + OT_D	UV + OV + OL_D + OT_D	OV + OL_D + OT_ND + OT_D	OV + OL_D + OT_ND + OT_D	UV + OV + OL_D + OT_D
RN 10	PV0												
	PV1	-	-	-	-	-	-	-	-	-	-	-	-
	PV2	-	-	-	-	-	-	-	-	-	-	-	-
	PV3	-	-	-	-	-	-	-	-	-	-	-	-
RN 14	PV0												
	PV1				-	-	UV + OL_ND	-	UV	UV + OL_ND	UV	UV	UV + OL_ND
	PV2				-	-	UV + OL_ND	-	UV	UV + OL_ND	UV	UV	UV + OL_ND
	PV3				OL_D	UV + OL_D	UV + OL_ND + OL_D	OL_D	UV + OL_D	UV + OL_ND + OL_D	UV + OL_D	UV + OL_D	UV + OL_ND + OL_D

FIGURE 10 | Classification of the type of criticality (OL, OV, UV) for the same networks and scenarios considered in Figure 9.

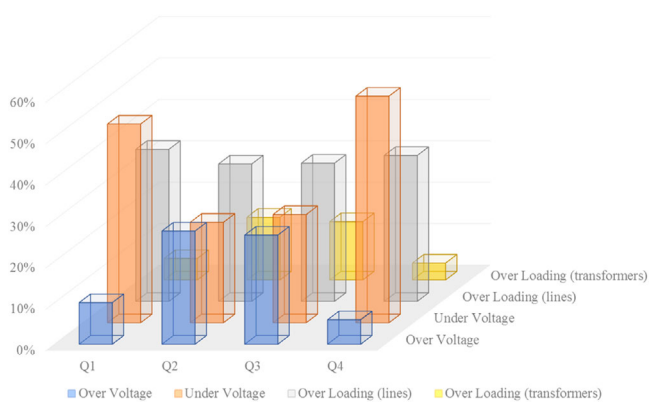

FIGURE 11 | Identified criticalities.

4.2 | Flexibility Assessment Results

Accordingly, with step 5 of the proposed approach (Section 3), the proposed assessment focuses on flexibility from load modulation and distributed generation control/curtailment. Flexibility contributions from EV smart charging and static energy storage are not explicitly represented; however, they could be considered without losing generality. Consequently, since PV generation is supposed to inject active power at a unitary power factor, reactive power variations arise solely from variations in the active demand power, assuming no deviation in the power factor. In the case study proposed in this paper, the maximum participation of the flexibility providers is described as follows:

- Active customers agree to reduce their consumption by a certain percentage (i.e., up to 50%).
- Producers, owners of renewable generators (i.e., PV systems), agree to curtail their production until they are shut down.

For active customers, a reduction of up to 50% is applied to the hourly baseline demand derived from each customer's load profiles, and it is assumed to be sustainable over the entire one-hour interval, without modelling rebound effects.

The assumed maximum load reduction of 50% is consistent with values reported in the demand response literature, where load reduction ratios between 10% and 50% have been documented for residential and commercial customers for HVAC-based strategies [27], while lighting in office buildings can achieve a load reduction ratio of up to 80% during peak hours, with an average daily value of 20% [28]. In addition, field trials in European residential settings have reported achievable household demand reductions of up to 33% during peak hours through automated demand response and home energy management systems [29]. In this context, the 50% value adopted in this work should be interpreted as an illustrative upper-bound assumption for flexibility activation, introduced to explore the network response under a sufficiently wide range of demand modulation levels. For PV generators,

		00:00	01:00	02:00	03:00	04:00	05:00	06:00	07:00	08:00	09:00	10:00	11:00	12:00	13:00	14:00	15:00	16:00	17:00	18:00	19:00	20:00	21:00	22:00	23:00
Q1	WORKING DAY	100	100	100	100	100	100	100	100	100	100	100	100	80	100	100	100	100	100	100	100	100	100	100	100
	PRE-HOLIDAY	100	100	100	100	100	100	100	100	100	100	100	100	40	100	100	100	100	100	100	100	100	100	100	100
	HOLIDAY	100	100	100	100	100	100	100	100	100	100	100	100	80	100	100	100	100	100	100	100	100	100	100	100
Q2	WORKING DAY	100	100	100	100	100	100	100	100	100	100	100	0	0	0	0	20	100	100	100	100	100	100	100	100
	PRE-HOLIDAY	100	100	100	100	100	100	100	100	100	100	100	0	0	0	0	20	100	100	100	100	100	100	100	100
	HOLIDAY	100	100	100	100	100	100	100	100	100	100	100	0	0	0	0	20	100	100	100	100	100	100	100	100
Q3	WORKING DAY	100	100	100	100	100	100	100	100	100	100	100	0	0	0	0	80	100	100	100	100	100	100	100	100
	PRE-HOLIDAY	100	100	100	100	100	100	100	100	100	100	100	0	0	0	0	20	100	100	100	100	100	100	100	100
	HOLIDAY	100	100	100	100	100	100	100	100	100	100	100	0	0	0	0	100	100	100	100	100	100	100	100	100
Q4	WORKING DAY	100	100	100	100	100	100	100	100	100	100	100	100	100	100	100	100	100	100	100	100	100	100	100	100
	PRE-HOLIDAY	100	100	100	100	100	100	100	100	100	100	100	100	100	100	100	100	100	100	100	100	100	100	100	100
	HOLIDAY	100	100	100	100	100	100	100	100	100	100	100	100	100	100	100	100	100	100	100	100	100	100	100	100

FIGURE 12 | Upward feasible flexibility of one RN-scenario combination.

the maximum downward modulation in each hour is equal to the instantaneous PV output given by the production profiles, so that the available downward flexibility naturally follows the diurnal and seasonal pattern of solar generation. Full curtailment is technically feasible with modern inverters and consistent with current regulatory practices, as MV-connected generators are already required to enable remote active power limitation by the DSO, and similar provisions are foreseen at the European level through flexible connection agreements [30].

By summarising these assumptions, the feasibility of the working points corresponding to the maximum reduction of the demand with the expected production (upward flexibility) and the maximum generation curtailment with the expected demand (downward flexibility) is checked and possibly scaled for finding the final percentage of demand reduction or production curtailment that the real networks, represented by the RNs under study, can offer to the MV.

Feasible flexibility is evaluated for all RN-scenario combinations, considering both configurations that remain compliant without reinforcement and those in which the identified reinforcements are applied to remove technical violations. Regarding networks that do not require reinforcement to address criticalities that may arise in future years, downward feasible flexibility is always the maximum potential. Thus, the network operation can tolerate production curtailment during all the typical days. On the contrary, upward feasible flexibility does not reach its maximum, and in some cases, it is null. In particular, upward feasible flexibility increases in versions of RNs with high demand (e.g., in the third class), but demand cannot be reduced at some hours of the day. Figure 12 illustrates this behaviour in one of those RNs, considering the highest increase in conventional load demand and HCS penetration, together with a high PV growth scenario. In the central hours of the day in Q1 and Q2, no upward flexibility can be provided (red area), whereas in Q1 at noon and in Q2 and Q3 at 3 p.m., up to 80% of the potential upward flexibility can be delivered. In all the remaining hours, 100% of the upward flexibility is feasible (green area), meaning that a curtailment of up to 50% of the load demand can be tolerated.

The time-dependent behaviour observed for the individual RN-scenario combinations can be extended to the full set of RNs that do not require reinforcement. In these networks, downward flexibility is always fully feasible (i.e., equal to 100% of the available potential in both 2030 and 2050). Upward flexibility, instead, may become more restrictive in specific simulated hours. Table 3 summarises this behaviour by classifying the substations according to the minimum feasible upward flexibility reached over the simulated typical days and hours. More specifically, the first class includes networks that reach 0% upward flexibility in at least one time interval, the second includes networks whose minimum feasible upward flexibility lies between 0% and 100%, and the third includes networks that maintain 100% upward flexibility throughout all simulated conditions. In 2030, 41% of the compliant substations fall into the first class, 15% into the second, and only 44% into the third. In 2050, the share of substations maintaining full upward flexibility throughout all simulated conditions increases to 63%, while the share reaching zero upward flexibility in at least one interval decreases to 29%.

TABLE 3 | Feasible upward and downward flexibility by scenario horizon for networks without reinforcement.

		Upward		**Downward**
Minimum flexibility	0%	0% - 100%	100%	100%
2030	41%	15%	44%	100.00
2050	29%	2%	63%	100.00

The remaining resized networks, for which reinforcement solved the violations over the horizon years, are more likely to offer the maximum upward and downward potential flexibility. Only one RN, in three versions that integrate the highest level of foreseen PV, cannot provide the maximum possible reduction of demand during the central hours of typical spring and summer days. This corresponds to 142 secondary substations out of the ~12,000 in the region.

Based on the results, some remarks can be formulated to explain differences across scenarios and seasons. The observed differences are primarily driven by the interaction between (i) the temporal mismatch between demand and distributed generation, (ii) the penetration level and spatial allocation of DERs, and (iii) the intrinsic characteristics of the LV networks. First, seasonal effects are largely explained by the variability of PV generation and demand patterns. Overvoltage and thermal overloads predominantly occur in spring and summer, when high PV production coincides with relatively low daytime demand, leading to reverse power flows and voltage rise phenomena. Conversely, undervoltage conditions are more frequent in autumn and winter, when higher demand and lower PV output increase current flows and voltage drop along feeders. Second, scenario-dependent drivers are associated with the increasing penetration

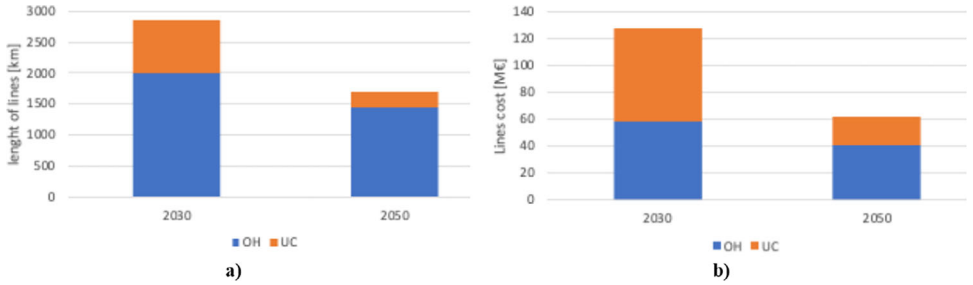

FIGURE 13 | a) Volumes (length of lines to be reinforced) and b) costs by line type (OH and UC) in the years 2030 and 2050.

TABLE 4 | Unitary costs.

Item	Costs
LV undergrounded cables—UC [€/km]	90,390
LV overhead cables – OH [€/km]	27,763
100 kVA LV/MV transformer [€]	7.300
160 kVA LV/MV transformer [€]	7,330
250 kVA LV/MV transformer [€]	7.660
400 kVA LV/MV transformer [€]	8.035
630 kVA LV/MV transformer [€]	9,540

of PV generation, HCS diffusion, and electrified loads. Higher PV levels amplify voltage rise and congestion issues, while increased demand and EV charging tend to exacerbate thermal loading and voltage drops. This explains the growing number and diversity of criticalities observed as penetration increases. Third, the results are strongly influenced by network structural characteristics, such as feeder length, load density, and transformer size. Networks with long feeders or low load density are more prone to voltage issues, whereas highly loaded or densely populated networks are more susceptible to thermal constraints. This heterogeneity explains why some representative networks remain compliant while others require reinforcement under the same scenario conditions. Finally, these drivers directly affect the feasibility of flexibility. Downward flexibility (e.g., PV curtailment) is generally unconstrained because it alleviates network stress, whereas upward flexibility (load reduction) is often limited, especially during periods of already low demand and high PV generation, when further reductions would worsen voltage rise conditions.

When mapped back to the real system, the reinforcement plan has been evaluated in terms of investments needed to bring the operation of future networks back within the technical constraints. More in detail, the unitary costs are reported in Table 4.

The final bill corresponds to an estimated expenditure of approximately 140 million euros in 2030 and 60 million euros in 2050 for line reinforcements (Figure 13b), and of roughly 20 million euros in 2030 and 35 million euros in 2050 for transformer replacements (Figure 14b). These outputs allow the DSO to compare reinforcement needs and their associated costs across scenarios and LV network classes. In this way, the technical analysis of LV criticalities is directly linked to the economic assessment of alternative planning options at the MV/LV interface. In terms of volumes, the LV reinforcements identified by the proposed procedure are not negligible. Most interventions concern overhead lines in rural and semi-urban areas. In contrast, a smaller number of underground cables in dense urban areas accounts for a disproportionate share of the cost due to much higher unit installation costs (Figure 13a). The cost of transformer replacements is a small, but still non-negligible, component of the overall expenditure, mainly driven by the uprating of existing 100–250 kVA units to the next standard size (Figure 14b).

4.3 | Computational Aspects

From a computational perspective, the proposed methodology is suitable for large-scale applications. In the case study, each hourly unbalanced power flow simulation with OpenDSS takes only fractions of a second on a standard workstation. Considering the typical Monte Carlo convergence range (10^3–10^4 iterations) and the full annual simulation horizon, a single RN–scenario combination can be analysed within times compatible with offline planning studies (from minutes to a few hours depending on the complexity and convergence speed).

The overall case study, including 16 representative networks and 469 RN–scenario combinations, was completed without requiring high-performance computing resources.

The computational burden scales approximately linearly with the number of representative networks, scenario combinations, and Monte Carlo samples. Moreover, the workflow is inherently parallelisable, as simulations for different RNs and scenarios are independent, enabling efficient execution on multi-core architectures or distributed/cloud environments.

5 | Conclusions

This paper proposes a methodology for evaluating the flexibility that LV networks can offer to the upper voltage level grids. The methodology employs synthetic network models to address the issues arising from the variety and large number of LV networks in a distribution system. Furthermore, the forecasted demand and generation patterns are downscaled to each secondary substation based on global projections formulated at national or regional levels. Then, to manage inherent uncertainties, a Monte Carlo approach is used to assess whether violations of technical

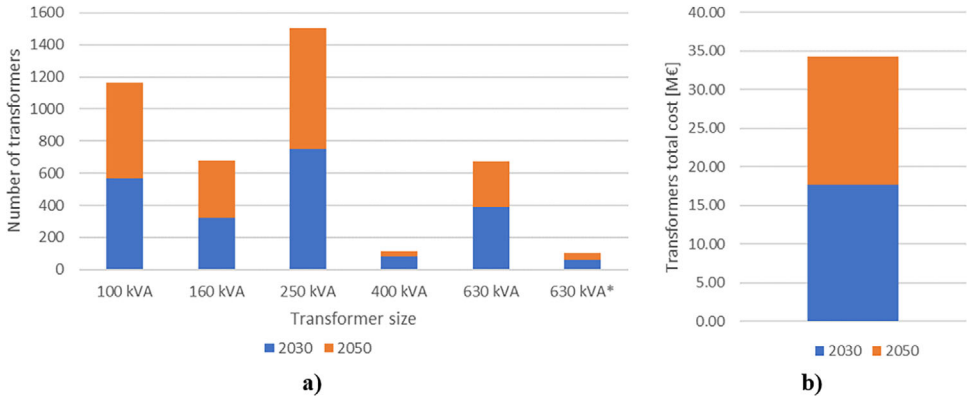

FIGURE 14 | a) Volumes (number of transformers to be substituted) by size and b) costs in the years 2030 and 2050.

constraints occur during the operation of the defined synthetic networks. Finally, the feasible flexibility is calculated for each version of the studied synthetic networks.

The case study demonstrates that LV constraints can substantially reduce the theoretically available flexibility, and this effect is strongly dependent on both the network type and the scenario combination. Some configurations remain compliant without any modification and can provide most of their potential flexibility, whereas others require targeted reinforcements before flexibility can be safely exploited. In this respect, the procedure not only identifies where LV constraints arise but also translates them into concrete upgrading needs on lines and transformers. The results indicate that LV reinforcements are not negligible, underlining that LV networks will increasingly influence the pace and cost of the energy transition, since most distributed resources and small flexibility providers are connected at this level.

Although a direct quantitative comparison with official reports or other studies is challenging because most available analyses estimate flexibility potential at aggregated levels (national, regional, or system-wide), whereas the proposed methodology evaluates flexibility at the MV/LV interface while explicitly considering LV network technical constraints, it is important to observe that the scenario assumptions adopted in this work are consistent with recent studies and official reports addressing the evolution of distribution systems under the energy transition (e.g., IEA [1, 2], Eurelectric [3]). These reports highlight the rapid growth of distributed renewable generation and electrified loads connected to distribution grids, as well as the growing importance of DER flexibility. At the same time, they emphasise that the effective exploitation of this flexibility depends strongly on the technical capabilities of distribution networks.

The results of this study confirm this trend, showing that LV network constraints, such as voltage limits and thermal loading of lines and transformers, can significantly reduce the theoretically available flexibility at the MV/LV interface under high-penetration scenarios of distributed resources. Such a reduction in the potential maximum flexibility offered by LV flexibility providers must be carefully considered by DSOs and TSOs that may need it. Future work will focus on coordinated distribution planning methodologies to realise development plans that exploit the benefits of flexibility without creating issues in LV networks.

Author Contributions

Fabrizio Pilo: funding acquisition, supervision, writing – review and editing. **Giuditta Pisano:** conceptualisation, data curation, formal analysis, investigation, methodology, validation, visualisation, writing – review and editing. **Simona Ruggeri:** conceptualisation, data curation, formal analysis, investigation, software, validation, visualisation, writing – original draft, writing – review and editing.

Acknowledgements

This work has been developed within the framework of the project. INS- Ecosystem of Innovation for Next Generation Sardinia (cod. ECS 00000038) funded by the Italian Ministry for Research and Education (MUR) under the National Recovery and Resilience Plan (NRRP)—MISSION 4 COMPONENT 2, 'From research to business' INVESTMENT 1.5, 'Creation and strengthening of ecosystems of innovation', and the construction of 'Territorial R&D Leaders'. This work benefited from technical discussions within the IEA Technology Collaboration Programme International Smart Grid Action Network (ISGAN), Working Group 3 (Cost-Benefit Analysis and Toolkits).

Open access publishing facilitated by Universita degli Studi di Cagliari, as part of the Wiley - CRUI-CARE agreement.

Conflicts of Interest

The authors declare no conflicts of interest.

Data Availability Statement

Data is subject to third-party restrictions.

References

1. IEA, *Renewables 2023 – Electricity* (International Energy Agency, 2023), https://www.iea.org/reports/renewables-2023/electricity.

2. IEA, *Global EV Outlook 2024* (International Energy Agency, 2024).

3. Eurelectric, "Grids for Speed – Executive Summary and Report," 2024. https://powersummit2024.eurelectric.org/wp-content/uploads/2024/05/Grids-for-Speed_Report.pdf.

4. G. Celli, G. Pisano, S. Ruggeri, et al., "Distribution Systems as Catalysts for Energy Transition Embedding Flexibility in Large-Scale Applications," *IEEE Access* 12 (2024): 92227–92240, https://doi.org/10.1109/ACCESS.2024.3421615.

5. J. Holweger, C. Ballif, and N. Wyrsch, "Distributed Flexibility as a Cost-Effective Alternative to Grid Reinforcement," *Sustainable Energy,*

Grids and Networks 34 (2023): 101041, https://doi.org/10.1016/j.segan.2023.101041.

6. F.-D. Martín-Utrilla, J. P. Chaves-Ávila, and R. Cossent, "Value of Flexibility Alternatives for Real Distribution Networks in the Context of the Energy Transition," *IEEE Access* 11 (2023): 114250–114269, https://doi.org/10.1109/ACCESS.2023.3322365.

7. European Parliament and Council, "Directive (EU) 2019/944 on Common Rules for the Internal Market for Electricity," *Official Journal of the European Union* 158 (June 2019): 125–199.

8. N. Natale, F. Pilo, G. Pisano, and G. G. Soma, "Quantitative Assessment of Flexibility at the TSO/DSO Interface Subject to the Distribution Grid Limitations," *Applied Sciences* 12, no. 4 (2022): 1858, https://doi.org/10.3390/app12041858.

9. G. Celli, G. Pisano, and S. Ruggeri, "Synthetic Representation of Flexibility From Aggregated LV Distributed Energy Resources," in *IET Conference Proceedings CP785* (The Institution of Engineering and Technology, 2021): 2925–2929.

10. A. Meletiou, J. Vasiljevska, and S. Vitiello, *DSO Observatory 2024 - Unlocking Flexibility in Europe*, JRC141953 (Publications Office of the European Union, 2025), https://doi.org/10.2760/7123923.

11. R. Monaco, C. Bergaentzlé, J. A. Leiva Vilaplana, E. Ackom, and P. S. Nielsen, "Digitalization of Power Distribution Grids: Barrier Analysis, Ranking and Policy Recommendations," *Energy Policy* 188 (2024): 114083, https://doi.org/10.1016/j.enpol.2024.114083.

12. X. Aldecoa, H. Zubia, A. Giménez, and I. López, "Enabling the Future: Digitalizing Low Voltage Networks and Enhancing Hosting Capacity Through Digital Twin," in *Proceedings of the CIRED 2024 Vienna Workshop* (IET, 2024), 76–79, https://doi.org/10.1049/icp.2024.1883.

13. L. De Vos, N. Leemput, N. Refa, R. Bernards, H. Fidder, and F. De Rijke, "Optimal Integration EV, PV, Heat Pumps in Existing Distribution Grids in the Netherlands," in *Proceedings of the 25th CIRED International Conference on Electricity Distribution* (CIRED, 2019), 3–6.

14. G. Pisano, N. Chowdhury, M. Coppo, et al., "Synthetic Models of Distribution Networks Based on Open Data and Georeferenced Information," *Energies* 12, no. 23 (2019): 4500, https://doi.org/10.3390/en12234500.

15. R. Vijay and P. Mathuria, "Feasibility and Flexibility Regions Estimation at TSO–DSO Interconnection Node Using Grid Structure Optimization," *Sustainable Energy, Grids and Networks* 32 (2022): 100952, https://doi.org/10.1016/j.segan.2022.100952.

16. A. Majumdar, O. Mousavi, T. Weckesser, F. Martins, and P. E. Sørensen, "Grid-Aware Provision and Activation of Fast and Slow Power Flexibility From Distributed Resources in Low and Medium Voltage Grids," *IET Generation, Transmission & Distribution* 17, no. 9 (2023): 2926–2937, https://doi.org/10.1049/gtd2.12686.

17. A. Rabiee, M. Marzband, and M. Fotuhi-Firuzabad, "Exploiting the Determinant Factors on the Available Flexibility Area of Active Distribution Networks at the TSO–DSO Interface," *IET Renewable Power Generation* 18, no. 3 (2024): 2455–2467, https://doi.org/10.1049/rpg2.13088.

18. B. R. Baecker, S. Candas, D. Tepe, and A. Mohapatra, "Generation of Low-Voltage Synthetic Grid Data for Energy System Modeling With the Pylovo Tool," *Sustainable Energy, Grids and Networks* 41 (2025): 101617, https://doi.org/10.1016/j.segan.2024.101617.

19. T. Lundblad, M. Taljegard, N. Mattsson, E. Hartvigsson, and F. Johnsson, "An Open Data-Based Model for Generating a Synthetic Low-Voltage Grid to Estimate Hosting Capacity," *Sustainable Energy, Grids and Networks* 39 (2025): 101483, https://doi.org/10.1016/j.segan.2024.101483.

20. A. Simonovska, V. Bassi, A. G. Givisiez, L. F. Ochoa, and T. Alpcan, "An Electrical Model-Free Three-Phase OPF for PV-Rich LV Networks Using Smart Meter and Transformer Data," *Electric Power Systems Research* 240 (2025): 111284, https://doi.org/10.1016/j.epsr.2024.111284.

21. G. Pisano, F. Pilo, and S. Ruggeri, "Predicting Flexibility From LV Networks by Using Geospatial Forecasting and Synthetic Networks," in *Proc. 28th Int. Conf. Exhib. Electricity Distribution (CIRED 2025), IET Conf. Proc.* (IET, 2025), 3264–3269, https://doi.org/10.1049/icp.2025.2423.

22. C. F. Heuberger, P. K. Bains, and N. M. Dowell, "Spatio-Temporal Optimisation Model to Investigate the Impact of Electric Vehicle Deployment," *Applied Energy* 257 (2020): 113715, https://doi.org/10.1016/j.apenergy.2019.113715, ISSN 0306–2619.

23. F. Pilo, G. Pisano, S. Ruggeri, and M. Troncia, "Data Analytics for Profiling Low-Voltage Customers With Smart Meter Readings," *Applied Sciences* 11 (2021): 500., https://doi.org/10.3390/app11020500.

24. IEA, *Electric Vehicle Charging and Grid Integration Tool*. 2023, https://www.iea.org/data-and-statistics/data-tools/electric-vehicle-charging-and-grid-integration-tool.

25. S. Conti, A. Melis, G. Pisano, F. Pilo, S. Ruggeri, and G. G. Soma, "Risk-Oriented Assessment of LV Distribution Network Hosting Capacity for Electric Vehicles," in *Proceedings of the CIRED 2024 Vienna Workshop: Increasing Distribution Network Hosting Capacity* (IET, 2024), 665–668.

26. R. L. Sellick and C. T. Gaunt, "Comparing Methods of Calculating Voltage Drop in Low Voltage Feeders," *Trans SAIEE* 86, no. 3 (September, 1995): 96–111.

27. K. O. Aduda, T. Labeodan, W. Zeiler, G. Boxem, and Y. Zhao, "Demand Side Flexibility: Potentials and Building Performance Implications," *Sustainable Cities and Society* 22 (2016): 146–163, https://doi.org/10.1016/j.scs.2016.02.011.

28. F. Sehar, M. Pipattanasomporn, and S. Rahman, "An Energy Management Model to Study Energy and Peak Power Savings From PV and Storage in Demand Responsive Buildings," *Applied Energy* 173 (2016): 406–417, https://doi.org/10.1016/j.apenergy.2016.04.039.

29. H. Aydin, E. Koçak, and S. Yılmaz, "Survey- and Simulation-Based Analysis of Residential Demand Response," *Sustainable Cities and Society* 96 (2023): 104678, https://doi.org/10.1016/j.scs.2023.104678.

30. European Parliament and Council, "Directive (EU) 2024/1711 of 13 June 2024 Amending Directives (EU) 2018/2001 and (EU) 2019/944 as Regards Improving the Union's Electricity Market Design," Official Journal of the European Union, L 2024/1711, 2024.